

Mixing Metals in the Early Universe

Andrea Ferrara¹, Max Pettini², & Yuri Shchekinov^{1,3}

¹Osservatorio Astrofisico di Arcetri, Firenze, Italy

²Institute of Astronomy, Madingley Road, Cambridge CB3 0HA, UK

³Department of Physics, Rostov State University, Rostov on Don, Russia

ABSTRACT

We investigate the evolution of the metallicity of the intergalactic medium (IGM) with particular emphasis on its spatial distribution. We propose that metal enrichment occurs as a two step process. First, supernova (SN) explosions eject metals into relatively small regions confined to the surroundings of star-forming galaxies. From a comprehensive treatment of blowout we show that SNa_e by themselves fail by more than one order of magnitude to distribute the products of stellar nucleosynthesis over volumes large enough to pollute the whole IGM to the metallicity levels observed. Thus, an additional (but as yet unknown) physical mechanism must be invoked to mix the metals on scales comparable to the mean distance between the galaxies which are most efficient pollutants. From this simple hypothesis we derive a number of testable predictions for the evolution of the IGM metallicity. Specifically, we find that: *(i)* the fraction of metals ejected over the star formation history of the universe is about 50% at $z = 0$; that is, approximately half of the metals today are found in the IGM; *(ii)* if the ejected metals were homogeneously mixed with the baryons in the universe, the average IGM metallicity would be $\langle Z \rangle = \Omega_Z^{ej} / \Omega_b \simeq 1/25 Z_\odot$ at $z = 3$. However, due to spatial inhomogeneities, the mean of the distribution of metallicities in the diffusive zones has a wide (more than 2 orders of magnitude) spread around this value; *(iii)* if metals become more uniformly distributed at $z \lesssim 1$, as assumed, at $z = 0$ the metallicity of the IGM is narrowly confined within the range $Z \approx 0.1 \pm 0.03 Z_\odot$. Finally, we point out that our results can account for the observed metal content of the intracluster medium.

Subject headings: Cosmology: theory – intergalactic medium – quasars: absorption lines

1. Introduction

Primordial nucleosynthesis enriched gas in the universe with the light elements He, D, and Li. It is only when the first galaxies and their stars appeared that heavier elements could be synthesized and, in some cases, ejected into the intergalactic medium. In currently popular

models of galaxy formation based on hierarchical clustering the first galaxies to form were low mass systems with such shallow potential wells that a few supernovae could deposit sufficient kinetic energy to expel the entire interstellar medium of the galaxy (Ferrara 1998). In this way, these initial episodes of star formation in the universe (sometimes referred to as Population III) may have enriched the intergalactic medium (IGM) to an average metallicity $Z_{\text{IGM}} \approx 10^{-4} Z_{\odot}$ (Miralda-Escudé & Rees 1997, Nath & Trentham 1997, Gnedin & Ostriker 1997, Ciardi et al. 2000b), comparable to that of the most metal-poor stars in the halo of our Galaxy (Ryan, Norris, & Beers 1996).

Most of the metals in the universe were presumably produced in larger collapsed structures at redshifts $z \lesssim 10$. In general such galaxies were better able to retain the products of stellar nucleosynthesis and could therefore achieve the abundance levels observed today. It is also likely that some metal-enriched gas escaped into the IGM, but it is far from clear by which process and to what degree the metals became distributed over large volumes, far from their production sites. These are the questions we consider in the present paper. Recent numerical hydrodynamic simulations of large-scale structure formation (Hellsten et al. 1997; Rauch et al. 1997; Zhang et al. 1998) have shown that baryons in the universe are distributed in a network structure (the “cosmic web”) with galaxies located at the high overdensity peaks. This implies that most of the volume is occupied by voids filled with gas at, or below, the mean cosmic density; such gas can be viewed as the long-sought-for true intergalactic medium. Since the voids are very large, with typical dimensions of several Mpc, their pollution by heavy elements produced in SN explosions is far from a trivial problem. In any case there must have been a protracted epoch when the metal content of the IGM was highly patchy.

Observationally, our best view of the IGM is still provided by the Ly α forest in the spectra of distant QSOs (Sargent et al. 1980) and the detection of metals in the forest ranks as one of the most significant discoveries made possible by the Keck telescopes (Cowie et al. 1995; Tytler et al. 1995). From an analysis of these data Hellsten et al. (1997) and Rauch, Haehnelt, & Steinmetz (1997) concluded that the measured column density ratios $N(\text{C IV})/N(\text{H I})$ imply that typically $[\text{C}/\text{H}] \simeq -2.5$ at $z \simeq 3$, with a one order of magnitude dispersion in the metallicity of different clouds about this mean value.¹ At lower redshifts ($z = 0.3 - 0.8$) Barlow & Tytler (1998) using HST/FOS spectra, with reasonable assumptions concerning the ionization correction and the line clustering properties, conclude that metallicities are as high as $[\text{C}/\text{H}] \gtrsim -1.3$, roughly an order of magnitude larger than the value at $z = 2.5$. These measurements, however, still refer to overdense regions of the universe, traced by Ly α clouds with column densities in excess of $\log N(\text{H I}) = 14.5$. The situation is far less clear-cut when we turn to the voids—or $\log N(\text{H I}) < 14.0$ —where the observations are very challenging even with a 10-m telescope. Two studies have addressed this problem, with conflicting results. Lu et al. (1998) applied a stacking technique to nearly 300 C IV regions in QSO spectra but still found no composite signal. They interpreted this non-detection

¹In the usual notation, $[\text{C}/\text{H}] = \log (\text{C}/\text{H}) - \log (\text{C}/\text{H})_{\odot}$.

as evidence for a highly non-uniform degree of metal enrichment at $z \simeq 3$, with the voids having $[C/H] \lesssim -3.5$. On the other hand, Cowie & Songaila (1998) used a pixel-to-pixel optical depth technique to conclude that the average C IV/H I ratio remains essentially constant over the full range of neutral hydrogen column densities tested, down to $\log N(\text{H I}) \simeq 13.5$. If this is indeed the case, the ejection and transport of metals away from galaxies must have been much more efficient than envisaged. Most recently, Ellison et al. (1999, 2000) have re-examined the problem and found that both approaches suffer from limitations which had not been properly taken into account in previous analyses. In their view, whether there are metals in the voids remains an open question.

On the theoretical side too, only a limited amount of work has been done on this topic. The common assumption that supernova driven winds may be able to distribute metals over large distances has been shown to be too simplistic and does not stand up to close quantitative scrutiny (MacLow & Ferrara 1999; Murakami & Babul 1999; D’Ercole & Brighenti 1999). These studies have come to the conclusion that efficient blowout is likely to be inhibited by the galaxy ISM and, at least at high redshift where densities are higher, by the pressure of the surrounding intergalactic gas (Babul & Rees 1992; Ciardi & Ferrara 1997). Gnedin & Ostriker (1998) numerically simulated the IGM enrichment in a CDM+ Λ cosmological model. They found that the mean metallicity of the universe at $z = 4$ is about $1/200 Z_{\odot}$ but the variations around this value are large and dependent on the overdensity. At this epoch the enrichment was incomplete, with some regions of the universe still of pristine composition. Their simulations, however, end at $z = 4$ so that a direct connection with the nearby universe is difficult. In addition, quantitative conclusions on the transport mechanism are affected by uncertainties arising from insufficient numerical resolution so that, for example, they are unable to resolve the snowplough phase of explosions. To alleviate the problem of inefficient blowout Gnedin (1998) developed the idea that metals are predominantly transported following merger events, a mechanism which would also predict a highly inhomogeneous distribution of heavy elements in the IGM at $z = 4$. However, the merger history has not yet been followed to more recent epochs.

In this paper we make explicit predictions for the IGM metallicity evolution by suggesting a two-step mechanism for the transport and mixing of heavy elements. In our scenario, SN explosions first eject metals over a relatively small region in the surroundings of the host galaxy; subsequently, a yet unknown diffusion process transports and mixes these elements over much larger scales. The plan of the paper is as follows. In §2 we consider the conditions for gas ejection from galaxies, paying particular attention to the treatment of blowout, which we show to be quite a rare occurrence in massive galaxies. In §3 we explicitly derive the metallicity evolution of the IGM for a particular (Cold Dark Matter) cosmological model. The results are discussed in §4 and a brief summary (§5) concludes the paper.

2. Metal Ejection by Galaxies

It is likely that the first episodes of star formation in the universe had a dramatic impact on the small mass galaxies in which they occurred. The combined effects of supernova explosions in relatively small volumes lead to the formation of superbubbles (SBs) which can result in partial (blowout) or even complete (blowaway) removal of the interstellar medium (Kovalenko & Shchekinov 1985; MacLow & McCray 1988; Ciardi & Ferrara 1997; Ferrara 1998; MacLow & Ferrara 1999). The resulting large scale outflows (galactic superwinds) have been observed directly in local starbursts (González Delgado et al. 1998; Heckman et al. 1998) and in Lyman break galaxies at $z \simeq 3$ (Lowenthal et al. 1997; Franx et al. 1997; Pettini et al. 1998; Pettini et al. 2000). For the purpose of this paper, we are interested in establishing the maximum galactic mass which allows blowout to occur. MacLow & Ferrara (1999) have shown that when blowout does take place the escape efficiency of the metals produced by the supernova progenitors is close to unity.

2.1. Conditions for Blowout

The blowout condition can be derived by comparing two characteristic velocities: the blowout velocity, v_b , and the escape velocity of the galaxy, v_e . To calculate these two velocities we start by defining a protogalaxy as a two component system consisting of a dark matter halo and a gaseous disk. We assume a modified isothermal halo density profile $\rho_h(r) = \rho_c/[1 + (r/r_a)^2]$ extending out to a radius $r_{200} \equiv r_h = [3M_h/4\pi(200\rho_{crit})]^{1/3}$, defined as the radius within which the mean dark matter density is 200 times the critical density $\rho_{crit} = 3H_0^2(1+z)^3/8\pi G$ at the redshift z when the halo is identified. M_h is the halo mass and $H_0 = 100h \text{ km s}^{-1} \text{ Mpc}^{-1}$ is the present-day Hubble constant; throughout this paper we adopt $\Omega = 1$.

For such a halo the escape velocity can be written as

$$v_e^2 \simeq 4\pi p G \rho_c r_a^2 = \frac{2pGM_h}{r_h}, \quad (1)$$

with $p = 1.65$ (MacLow & Ferrara 1999). Note that $v_e = \sqrt{2p} v_c$, where v_c is the circular velocity of the halo.

Due to the dissipative nature of the gas, the baryons which initially should be distributed approximately as the dark matter, will lose pressure and collapse in the gravitational field of the dark matter. The density ratio between these two components is assumed here to be equal to its cosmological value, and therefore the initial density of the gas in the protogalaxy is $\rho_g = \Omega_b \rho_h$. If the halo is rotating, the gas will collapse in a centrifugally supported disk. The radius of the disk can be estimated by imposing that the specific angular momentum of the disk, j_d , is equal to that of the halo, j_h (Mo et al. 1998, Weil et al. 1998)

$$j_h = \sqrt{2}\lambda v_c r_h = 2v_c \ell_d = j_d \quad (2)$$

where ℓ_d is the disk scale length and λ the standard halo spin parameter. As shown by numerical simulations (Barnes & Efstathiou 1987; Steinmetz & Bartelmann 1995) λ depends very weakly on M_h and on the density fluctuation spectrum; its distribution is approximately log-normal and peaks around $\lambda = 0.04$. From eq. 2 we then obtain $\ell_d = (\lambda/\sqrt{2})r_h$. For an exponential disk, implicitly assumed in deriving eq. 2 above, the optical radius (*i.e.* the radius encompassing 83% of the total integrated light) is $3.2 \times \ell_d$. Since galaxies typically extend ≈ 2 times their optical radius in H I (Salpeter & Hoffman 1996), we adopt for the radius of the gaseous disk

$$r_d = 4.5\lambda r_h. \quad (3)$$

We now evaluate the scale height of the gas in the disk. This is roughly given by

$$H \simeq \frac{c_s^2 r_d^2}{GM_h} \simeq 70\lambda^2 \left(\frac{c_s}{v_e}\right)^2 r_h \quad (4)$$

where we have used the expression for r_d above; c_s is the effective gas sound speed which also includes a possible turbulent contribution. Note that

$$\frac{H}{r_d} = 15.3\lambda \left(\frac{c_s}{v_e}\right)^2 \quad (5)$$

If all baryons bound to the dark matter halo were able to collapse, the mean gas density in the disk would be

$$\rho_d \approx \left(\frac{r_h}{r_d}\right)^3 \left(\frac{r_d}{H}\right) \rho_g. \quad (6)$$

The previous assumption, although uncertain, gives approximately the correct density when scaled to Milky Way parameters; in addition, ρ_d enters in the expression for v_b below to the 1/3 power. Thus, unless the fraction of collapsed baryons is unreasonably low, a value lower than unity does not lead to qualitatively different conclusions. The explicit expression for the blowout velocity, v_b , has been obtained by Ferrara & Tolstoy (2000):

$$v_b = 2.7 \left(\frac{L}{\rho_d H^2}\right)^{1/3}, \quad (7)$$

where L is the mechanical luminosity of the parent SB. Note that v_b by definition (Ferrara & Tolstoy 2000) is estimated at a height equal to $3H$ above the galactic plane. Obviously, if the blowout velocity has already decreased below the local sound speed at that point, the blowout is inhibited. By using eqs. 3, 6 and 4 it is easy to show that $H^2 \rho_d \propto \Omega_b c_s^2$, that is the product $H^2 \rho_d$ is independent of mass and redshift; therefore v_b depends on these quantities only through L . Blowout occurs if $v_b > v_e$, or

$$2.7 \left(\frac{L}{H^2 \rho_d}\right)^{1/3} \geq \left(\frac{2pGM_h}{r_h}\right)^{1/2}. \quad (8)$$

This implies that the mechanical luminosity for a SB to blowout must be larger than the critical value

$$L_c = (0.27pG)^{3/2} \rho_d H^2 \left(\frac{M_h}{r_h}\right)^{3/2}. \quad (9)$$

The *total* mechanical luminosity of the corresponding SB in a primordial galaxy that virialized at redshift z can be written as (Ferrara 1998)

$$L_t(z) = \epsilon_0 \nu \dot{M}_\star = \frac{\epsilon_0 \nu \Omega_b f_b}{\tau_\star t_{ff}(z)} M_h, \quad (10)$$

where $\epsilon_0 = 10^{51}$ ergs is the energy of a SN explosion and \dot{M}_\star is the star formation rate; we assume a Salpeter IMF, for which one SN is produced for each $56 M_\odot = \nu^{-1}$ of stars formed. The baryon density parameter is $\Omega_b = 0.05 \Omega_{b,5}$, of which a fraction $f_b \sim 0.08 f_{b,8}$ (Ciardi et al. 2000a) is able to cool and become available to form stars. The free-fall time is $t_{ff} = (4\pi G \rho_h)^{-1/2}$; $\tau_\star^{-1} = 3\%$ is the star formation efficiency, which is fixed by matching to the cosmic star formation history as described in §4.2 below.

For Population III objects, which as we have argued are likely to have been of low mass, we make the simplifying assumption that star formation is confined to a relatively small region, and that all the exploding SNaes associated with the initial star formation episode result in the formation of a single superbubble. In this case a comparison between eq. 9 and eq. 10 shows that $L_t(z)/L_c$ does not depend on mass and redshift, and the condition $L_t(z) > L_c$ is satisfied when

$$\frac{\epsilon_0 \nu f_b}{\tau} > 0.1 c_s^2, \quad (11)$$

which for typical parameters is equivalent to $4.4 \times 10^{12} > 0.1 c_s^2$, and is therefore valid for galaxies with $c_s \leq 70$ km/s. Thus low mass galaxies with coherent star formation (*i.e.* with all SNaes driving a single SB) are very likely blowing out.

For more massive and larger galaxies we have to consider the more realistic situation where the SNaes are more widely distributed within the disk, and occur in OB associations with different values of L_{OB} (or, equivalently, with a different number N of SNaes). In nearby galaxies it is found that the luminosity function of OB associations is well approximated by a power-law

$$\phi(N) = \frac{d\mathcal{N}_{OB}}{dN} = AN^{-\beta} \quad (12)$$

with $\beta \approx 2$ (McKee & Williams 1997; Oey & Clarke 1998). Here \mathcal{N}_{OB} is the number of associations containing N OB stars; normalization of $\phi(N)$ to unity requires $A = 1$. Thus the probability for a cluster of OB stars to host N SNaes is $\propto N^{-2}$, where $N = L_{OB} t_{OB} / \epsilon_0$, and $t_{OB} = 40$ Myr is the time at which the lowest mass ($\approx 8 M_\odot$) SN progenitors expire. The total mechanical luminosity, which must be equal to $L_t(z)$ in eq. 10, is then found to be

$$L_t(z) = \int_{N_m}^{N_M} L_{OB}(N) \phi dN, \quad (13)$$

where $N_m = 1$ (N_M) is the minimum (maximum) possible number of SNaes in a cluster. This gives

$$L_t(z) = \text{const.} \frac{\epsilon_0}{t_{OB}} \ln \frac{N_M}{N_m}. \quad (14)$$

The contribution to the total luminosity from clusters powerful enough to lead to blowout is

$$L_B(z, > L_c) = \text{const.} \frac{\epsilon_0}{t_{OB}} \ln \frac{N_M}{N_c}, \quad (15)$$

where N_c is the number of SNae in a cluster with mechanical luminosity equal to L_c , i.e.

$$N_c = \frac{L_c t_{OB}}{\epsilon_0}. \quad (16)$$

Thus, the fraction of the mechanical energy which can be blown out is

$$\delta_B = \frac{\ln(N_M/N_c)}{\ln(N_M/N_m)} < 1. \quad (17)$$

Clearly, N_M (and therefore δ_B) is an intrinsically stochastic number. To determine its dependence on the total number of supernovae $N_t = L_t(z)t_{OB}/\epsilon_0$ produced by a galaxy during the lifetime of an OB association, we have used a Monte Carlo procedure applied to the distribution function in eq. 12. The results for N_M and δ_B as a function of N_t are shown in Fig. 1; we recall that the star formation rate \dot{M}_\star in the galaxy is related (through eq. 10) to N_t by $\dot{M}_\star \approx 5 \times 10^{-6} N_t M_\odot \text{ yr}^{-1}$. As can be seen from Fig. 1, for low values of N_t the quantity N_M is larger than N_c , implying that in every galaxy at least some SBs are able to blow out. However, near $N_t = 10^4$ N_M flattens and eventually becomes equal to N_c at $N_t \simeq 45\,000$. Above this limit (corresponding to a galaxy with $\dot{M}_\star \approx 0.35 M_\odot \text{ yr}^{-1}$ or $M_h \approx 10^{12}(1+z)^{-3/2} M_\odot$) blowout is inhibited. The fraction δ_B can be seen from Fig. 1 to be a decreasing function of N_t ; an approximate analytical form is

$$\begin{aligned} \delta_B(N_t) &= 1 \quad \text{for } N_t < 100 \\ \delta_B(N_t) &= a + b \ln(N_t^{-1}) \quad \text{for } N_t > 100, \end{aligned} \quad (18)$$

with $a = 1.76$, $b = 0.165$. Clearly, in small galaxies even the smallest associations are capable of producing blowout, so that the issue of coherence discussed above is irrelevant.

Thus, if we assume the most of the baryonic matter has collapsed into the disk, the main metal polluters of the IGM at the present epoch are galaxies with visible mass lower than $M_d^{up} = \Omega_b M_h \lesssim 5 \times 10^{10} M_\odot$. This critical mass decreases with increasing redshift as $(1+z)^{-3/2}$, indicating that the initial metal enrichment of the universe must have been produced by even smaller galaxies. For example, at $z = 20$, the expected value of M_d^{up} is only $5 \times 10^8 M_\odot$.

2.2. Confinement of Blowout-driven Outflows

Blowout will drive an outflow which will eventually be confined by the IGM pressure. What is the characteristic length, R_e , at which such pressure equilibrium is achieved? By requiring that the outflow ram pressure, $\rho_w v_w^2$, is equal to the IGM pressure, p_i we obtain

$$R_e = \left(\frac{\dot{M}_w v_w}{4\pi p_i} \right)^{1/2}; \quad (19)$$

where we have used mass conservation and assumed that the flow is approximately spherical. Once recombination is complete at redshift $z \approx 200$, and before the IGM is reheated by the energy input from the first galaxies, the IGM pressure will evolve almost adiabatically, $p_i = p_*[(1+z)/200]^5$, where $p_*/k_B \approx 1500h^2 \text{ cm}^{-3} \text{ K}$ is the value of p_i at $1+z=200$. However, almost unavoidably, even the earliest SN-driven bubbles will expand in an IGM which has been pre-ionized by the same massive stars which later exploded as SNaE. Thus, it seems more appropriate to calculate the IGM pressure in the surroundings of the galaxy as $p_i = (R/\mu)\rho_i(z)T$, with $T \approx 2 \times 10^4 \text{ K}$ as a result of photoionization heating. This is a reasonable hypothesis since it can be shown (Ciardi et al. 2000a) that the ionization spheres are much larger than the metal-enriched bubbles considered here. The mass loss rate \dot{M}_w is typically a fraction $\xi \approx 10\%$ of the star formation rate $\dot{M}_* = L_e/\epsilon_0\nu$ (Ferrara & Tolstoy 2000) where $L_e = \delta_B L_t$ is the effective mechanical luminosity, that is the fraction available for blowout; we can also assume that $v_w \simeq v_e$. With these hypotheses, and using the relations derived above for v_e , one obtains

$$R_e(M_h, z) = 0.9 \left(\frac{\Omega_{b,5} v_e^4 \delta_B}{\lambda_4 p_i} \right)^{1/2} \text{ cm}, \quad (20)$$

where $\lambda_4 = \lambda/0.04$. The behavior of R_e with M_h is shown in Fig. 2 for different redshifts. At lower redshifts, the bubbles are larger because the pressure of the confining IGM is lower; also evident from the figure is the increase of the critical mass for blowout with decreasing z .

The major conclusion that can be drawn from Fig. 2 is that supernova-driven outflows are quite inadequate for dispersing heavy elements far from their production sites and cannot account, by themselves, for the ubiquitous presence of metals in the IGM at $z \simeq 3$. This can be readily realized when we consider that in standard Cold Dark Matter models, taken here as representative of a larger class of hierarchical models of structure formation, the typical (physical) separation between objects with mass $M_h \approx 10^{10} M_\odot$ varies between 2 – 0.2 Mpc in the interval $0 < z < 8$ (Ciardi et al. 2000a). This scale is much larger than the values of R_e in Fig. 2, so that we would expect regions outside the metal enriched bubbles to retain their primordial composition (this argument is reconsidered more rigorously in §4 below). Clearly some other mechanism must be operating to remove the metals from the surroundings of galaxies and mix them with the more generally distributed IGM.

3. Predictions for CDM Models

To make further progress, we need to fix a specific cosmological model. As an example, we consider the so-called Standard Cold Dark Matter (SCDM), with $\Omega_M = 1, \Omega_\Lambda = 0$, and $h = 0.5$; the power spectrum $|\delta_k|^2$ is taken from Efstathiou et al. (1992), normalized to the present-day abundance of rich clusters ($\sigma_8 = 0.6$; Eke, Cole, & Frenk 1996). To calculate the number density of dark matter halos as a function of redshift we use the Press & Schechter (1974, hereafter PS) formalism; this technique is widely used in semi-analytical models of galaxy formation and

gravitational lensing (White & Frenk 1991, Kauffman 1995, Ciardi & Ferrara 1997, Baugh et al. 1998, Guiderdoni et al. 1998, Marri & Ferrara 1998) and it has been shown to be in surprisingly good agreement with the results from N-body numerical simulations. Given a power spectrum $|\delta_k|^2$, one can write the Gaussian variance of the fluctuations on the mass scale M :

$$\sigma_M^2 = \int \frac{d^3k}{(2\pi)^3} W^2(k, R) |\delta_k|^2, \quad (21)$$

where $M = (4/3)\pi\rho R^3$, ρ is the matter density, and

$$W = \frac{3}{(kR)^3} [\sin(kR) - (kR) \cos(kR)]; \quad (22)$$

is a top-hat filter function. From the results of the nonlinear theory of gravitational collapse, stating that a spherical perturbation with overdensity $\delta_c = \delta\rho/\rho > 1.69$ with respect to the background matter collapses to form a bound object, through the PS formalism we can derive the normalized fraction of collapsed objects per unit mass at a given redshift:

$$f(M, z) = \sqrt{\frac{2}{\pi}} \frac{\delta_c(1+z)}{\sigma_M^2} e^{-\delta_c^2(1+z)^2/2\sigma_M^2} \left(-\frac{d\sigma_M}{dM} \right). \quad (23)$$

Then the comoving number density of dark matter halos per unit mass is

$$n_h(M_h, z) = \frac{\Omega_M \rho_{crit}}{M} f(M_h, z). \quad (24)$$

We can now ask what is the fraction of the IGM polluted by metals at different redshifts. To this end we calculate an IGM porosity parameter, $Q(z)$, defined by

$$dQ(z) = M_h \left| \frac{dn_h}{dz} \right| R^3(M_h, z) dz, \quad (25)$$

in two different cases. First, we consider the case in which metals are only injected in the IGM by superbubbles and therefore $R \equiv R_e$ in the previous equation. The resulting porosity evolution (complete overlap of the bubbles occurs for $Q = 0.16$, Smith 1976) is shown in Fig. 3. Again we see that blowout by itself would lead only to a negligible dispersal of metals ($Q < 10^{-4}$), with most of the IGM maintaining its primordial composition to the present day.

If we are to explain the relatively ubiquitous presence of metals in the ‘true’ IGM, as deduced from at least some observations, we are then forced to assume that some additional physical mechanism, capable of efficiently transporting metals away from their production sites, must be at work. The nature of such a process can only be matter of speculation at present, because neither the numerical simulations nor the observations have yet reached the required levels of sophistication or sensitivity to address this question properly. Among the options which are worth exploring are galaxy collisions, diffusive processes and the peculiar motions of galaxies. We consider the relative importance of these different possibilities in future work.

Here we take a strictly phenomenological approach which nevertheless has considerable predicting power. We introduce a diffusive radius, R_d , defined as the mean interdistance between the galaxies responsible for providing the predominant contribution to the metal enrichment of the IGM (see Fig. 4), *i.e.* $R_d = 0.2$ Mpc (comoving) for $M_h > 2 \times 10^8 M_\odot$. As the largest Doppler parameters measured in Ly α clouds are of order ≈ 50 km s $^{-1}$, the time required for a pollution front to travel such a distance is shorter than the Hubble time only at redshifts $z < 1$. Thus, our assumption is equivalent to fixing at $z \lesssim 1$ the epoch at which metals become homogeneously distributed. As we will see shortly, this simple hypothesis leads to a number of consequences which are in accord with available data. If future studies of possible mechanisms for the diffusion of metals are able to determine directly the value of R_d and its evolution with time, it will be relatively easy to include their results in the general framework of this paper and explore any differences with the conclusions presented here.

As can be seen by Fig. 3, when the condition $R = \max(R_e, R_d)$ is introduced, mixing is improved dramatically—as expected, and metal-enriched bubbles indeed overlap at $z \approx 1$. At later epochs essentially all of the IGM is polluted with heavy elements produced in galaxies and subsequently redistributed by the combined effects of blowout and diffusion.

3.1. Metallicity of Polluted Regions

We can now calculate the average metallicity of the gas inside the diffusive spheres. In order to do so we need to know μ_Z , the mass of metals produced by the typical supernova. Nucleosynthesis calculations in Type II SNaE by Tsujimoto et al. (1995) predict $\mu_Z \approx 2 - 3M_\odot$ for a Salpeter IMF, depending on the upper mass limit above which a black hole is formed. Here we adopt $\mu_Z = 2.58M_\odot$, also consistent with a matching to the cosmic star formation history (§4.2). By design, mixing is efficient and the metal distribution is therefore homogeneous within the radius R_d . The total number of SNaE per galaxy is

$$\mathcal{N}_{SN} = \frac{\nu\Omega_b f_b}{\tau_\star} M_h. \quad (26)$$

Then the mass of metals ejected by a galaxy inside a halo of mass M_h is

$$M_e = \frac{\mu_Z \nu \Omega_b f_b}{\tau_\star} M_h \delta_B, \quad (27)$$

with δ_B given by eq. 18. The metal density in a diffusive sphere surrounding a given halo is $\rho_Z = 3M_e/4\pi R_d^3$, and its average metallicity is $\rho_Z/\rho_i(z)$, where $\rho_i(z)$ is the mean density of IGM at redshift z . This assumption restricts our analysis to the case of the ‘true’ IGM, characterized by overdensities close to unity. Extrapolation of the results to hydrogen column densities $\log N_{HI} \gtrsim 14$ is only very qualitative and deserves more study. The dependence of metallicity in the diffusive spheres on halo mass and redshift is plotted in Fig. 4. At any given redshift, Z increases as a function of mass (because of the increasing metal production) up to an abrupt cutoff

when blowout becomes inhibited, as described by the behavior of δ_B in Fig. 1. As the spheres grow with time, the metals are distributed over larger volumes and this is reflected by the shift to lower metallicities with decreasing z in Fig. 4. Note that for the same reason pockets of very high metal content ($Z \approx 1Z_\odot$) are expected at large z , although the size of these regions is very small.

3.2. IGM Metallicity Evolution

Once the cosmological model has been fixed, we need to determine the values of the the star formation efficiency, τ_\star , in order to calculate the metallicity of the IGM as a function of time. We choose this value by comparison with observations, as follows. We calculate the evolution of Ω_\star , the density parameter of stars formed in the universe (see Fig. 5), with the requirement that at $z = 0$ it matches the estimate by Fukugita, Hogan & Peebles (1998). These authors conclude that $\Omega_\star(0)$ in spheroids, disks and irregulars is $\approx 0.0049h_{50}^2$. A similar value is found by integrating current estimates of the star formation rate density in the universe as a function of redshift, as deduced from deep imaging surveys (Pettini 1999). With this normalization (giving $\tau_\star^{-1} \approx 3\%$), we can then derive the corresponding evolution of the metals produced by stars and returned to the ISM Ω_Z (Fig. 5), which is directly proportional Ω_\star .

However, not all the metals can escape from the galaxy where they have been produced. The cosmic ejection fraction, $f_{ej}(z)$, (*i.e.* the ejection fraction averaged over the entire population of halos) is very close to unity at high redshift where predominantly small galaxies are present, but it steadily decreases to about 50% at $z = 0$, as the number of more massive galaxies able to retain their metals increases. For this reason, the curve describing the density parameter of *ejected* metals $\Omega_Z^{ej} = f_{ej}(z)\Omega_Z(z)$ in Figure 5 progressively deviates from that for $\Omega_Z(z)$ with decreasing redshift. Stated differently, today about 50% of the metals produced should reside in the IGM. If the metals were homogeneously mixed with the baryons in the universe at any redshift the average IGM metallicity (top curve in Fig. 5) would be $\langle Z \rangle = \Omega_Z^{ej}/\Omega_b \simeq 1/25Z_\odot$ at $z = 3$ and $\langle Z \rangle \simeq 0.1Z_\odot$ at $z = 0$. Note that the average metallicity of today's galaxies would be higher by a factor $\Omega_b/(\Omega_\star + \Omega_g)$ (the baryon density divided by the sum of star and gas density in galaxies); we therefore expect that for luminous matter today $\langle Z \rangle \approx Z_\odot$, in accord with observational estimates (Edmunds & Phillips 1997).

Our main results are displayed in Figure 6 and 7, which show in the spread in metallicity as a function of redshift, compared with the average $\langle Z \rangle$ of the IGM from Figure 5. The two figures correspond to different metallicities of the outflowing hot gas in the superbubbles, assumed to be Z_\odot in Fig. 6 and $8Z_\odot$ in Fig 7. In the figures the metallicity distribution at each redshift considered is shown in the vertical direction with the density of symbols approximately proportional to the amplitude of the distribution. The distributions are relatively flat, but at redshifts $z \lesssim 5$ they also show a double-horned profile with points accumulating at the highest and lowest metallicities. We illustrate this effect in Figure 8, where we have reproduced the metallicity histograms at $z = 0$ and $z = 1$ from Figure 6. The more massive galaxies are responsible for the high metallicity peaks

in these distributions, caused by the cutoff in the ejection fraction described by the parameter δ_B (Figure 1). The low metallicity maximum is due to the increasing number of low mass halos.

There are several interesting features of Figures 6 and 7 which we now discuss briefly. First, at $z > 6$ the average IGM metallicity is not within the predicted ranges of metallicities, being lower than the lowest values in the distributions. What we are seeing is a highly inhomogeneous distribution of metals which are still clumped in small regions around the galaxies which produced them. As mixing proceeds, the average metallicity increasingly becomes a better description of the true mean metallicity, and approaches the mean of the distribution. At $z \approx 1$ the postulated diffusion leads to all the volume in the universe being polluted with heavy elements to some extent (Figure 3). The merging of the metal-enriched spheres produced by different galaxies has the effect of erasing regions of low metallicity: the minimum metallicity corresponds to that in spheres marginally overlapping at a given redshift. This effect is reflected in the growth of the lower boundary of the distributions from $(1+z) \lesssim 5$ in Figures 6 and 7, and results in the present-day IGM metallicity being confined within the narrow range $0.1 \pm 0.03 Z_\odot (1 \sigma)$.

The decreasing spread in metallicity with time is a direct result of the growth of $\langle Z \rangle$. At high z , where the overall level of enrichment is low, even relatively metal-poor spheres have a chance to stand out. However, as the average IGM metallicity increases, only a few massive objects are able to produce diffusive spheres with Z sufficiently high to be recognized as metallicity peaks (and still be able to eject their metals). The situation is similar to a “flooding effect”, where as the water level rises fewer and fewer mountain peaks can be seen.

At redshifts $z > 1$, when metal enrichment is highly inhomogeneous, a considerable fraction of the IGM is still of essentially primordial composition. Thus, at $z \approx 3$ for example, we expect that only some low column density Ly α forest clouds will show associated metal lines, while the majority will not; the ratio between Ly α clouds with and without metals depends on the covering factor of the diffusive spheres and grows with time. This has implications for the interpretation of the results of searches for metals in the forest. Given the low optical depths when $\log N(\text{H I}) < 14$, such searches are normally conducted in a statistical way, by considering together the data from many absorption lines. In such cases one obtains some gross average over all the absorbers which, given the dilution with the unpolluted IGM, will be systematically lower than the values of $\langle Z \rangle$ plotted in Figures 6 and 7. For this reason we also show in these figures the covering factor-weighted metallicity $\langle Z P(z) \rangle$, where $P(z)$ describes the evolution of the covering factor down to $z = 1$.

In Figures 6 and 7 we have used different symbols to represent the contributions to the IGM metallicity from halos with virial temperatures above (hexagons) and below (triangles) 10^4 K, to give a qualitative idea of the role of large and small objects in the enrichment process. It is seen that at high z small objects are controlling the process, whereas at lower redshift enrichment is largely regulated by more massive galaxies (up to the ejection limit set by δ_B , see Figure 3). If some inhibiting effect, such as photoheating by the UV background, affects preferentially low mass

galaxies, the lower metallicity bounds at high redshift will move up accordingly, shifting closer to the line separating hexagons from triangles. The flat upper boundary of the distribution at high z reflects the fact that the volumes involved are so small that the IGM baryon loading results in a negligible dilution of the metallicity of the ejecta. Since there is no firm measurement of this quantity at present (Heckman, private communication), we have considered two possibilities, Z_{\odot} (our standard case) and $8 Z_{\odot}$ in Figures 6 and 7 respectively. The IGM metallicity distribution is affected by this choice at high redshift, but the difference becomes much smaller at low z , where the IGM baryon loading regulates the dilution of the larger diffusive spheres.

Finally, we also show in the two figures the average metallicities for the case in which metal-enriched spheres with size below $R_e(min) = 1$ kpc have been excluded. In our models these are the absolute lower limits to the average IGM metallicity at a given redshift. $R_e(min)$ has been calculated by imposing the condition that the collisional timescale between galaxies with a given impact parameter is shorter than the Hubble time at any redshift up to $z = 10$. Obviously, a sphere with size greater than $R_e(min)$ can be strongly disturbed by tidal interactions following an encounter at greater impact parameter, and for this reason the curves obtained in this way are strictly lower limits. Nevertheless, as can be seen from Figure 6 and 7, imposing this condition reduces the metallicity by only about 40%.

In addition to the SCDM model, we have also considered a CDM model with a cosmological constant (CDM+ Λ) with $\Omega_M = 0.4, \Omega_{\Lambda} = 0.6, h = 0.5$). By normalizing the star formation rate following the same procedure as for the SCDM model we obtain a higher value of $\tau_{\star}^{-1} = 10.5\%$. Because of the normalization, the resulting metal distribution is qualitatively very similar to the one derived for the SCDM case. The only notable differences are a larger metallicity spread between $0.5 < z < 2$ and a somewhat higher mean value at $z = 0$, $\langle Z \rangle = 0.15 \pm 0.03 Z_{\odot}$.

4. Discussion

The basic conclusion of this paper is that metal ejection driven by SN events fails, by more than one order of magnitude, to distribute the products of stellar nucleosynthesis over volumes large enough to pollute the whole IGM to the typical metallicity of Ly α clouds, $[C/H] \simeq -2.5$. We are therefore forced to conclude that some additional physical process must be at play, the nature of which remains to be determined. In our scheme transport of metals occurs in two sequential steps. First, SNa e provide the initial kick necessary to eject heavy elements outside the potential well of a galaxy, but the ejecta are then confined by the IGM pressure to a relatively small bubble, of radius R_e . We then postulate that a second process is responsible for the diffusion of metals on a typical scale R_d , comparable to the mean distance between the galaxies which are the most efficient pollutants of the IGM.

Our scenario is qualitatively different from that proposed by Gnedin (1998), who attributed the mixing to more violent and rarer galaxy mergers. In the model proposed here SNa e are of

fundamental importance as they initiate the mixing process. However, galaxy collisions might well play a role in the subsequent phase during which metals are spread over larger scales, of order R_d . Other diffusive processes, such as thermal conduction and turbulent mixing layers at the interfaces between cosmological flows, as well as the peculiar motions of galaxies, may also be important in determining the spatial structure of the distribution of metals. A detailed study of such processes is beyond the scope of this paper and should, in any case, be based on cosmological simulations which are in progress. We will report of this extension of the work in a forthcoming paper.

In the present study we have stressed that the IGM enrichment proceeds in a very inhomogeneous manner, with pockets of metal rich gas gradually increasing both in number and in size until they overlap at $z \approx 1$. The average metallicity of the IGM increases with time, a trend confirmed by the results in Barlow & Tytler (1998), who found an order of magnitude increase in the metallicity of the Ly α forest between $z = 2.5$ and $z = 0.5$. Although our results are strictly applicable only to the ‘true’ IGM with overdensities close to unity, we nevertheless regard this as an encouraging performance of our model.

The metallicity spread is predicted to decrease with the progress of time. At $z \lesssim 1$, when the entire volume of the universe has been exposed to metal pollution, the spread in metallicity is less than one order of magnitude, and at the present epoch $\langle Z \rangle = 0.1 \pm 0.03 Z_\odot$. Thus we predict that at $z < 1$ essentially all absorbers should have associated C IV absorption, irrespectively of their column density. The effect should be very pronounced. Not only are the voids polluted by the overlap of metal-enriched diffusive spheres, as discussed above, but the decreasing intensity and hardness of the ionizing background lead to a further increase in the fraction of C which is triply ionized, so that the ratio $N(\text{C IV})/N(\text{H I})$ increases for a fixed [C/H] (Rauch et al. 1997). It should be possible to test these predictions with forthcoming observations. UV-efficient echelle spectrographs, now available on the VLT and soon on the Gemini South telescope, will allow sensitive searches for C IV doublets at significantly lower redshifts than probed so far, while STIS on *HST* and FUSE will map the Ly α forest with the required spectral resolution at wavelengths below 3000 Å, which are inaccessible from the ground.

While our study has concentrated on the IGM, it also has important consequences for the metallicity of the intracluster medium. which is found to have a rather uniform value $\approx 1/3 Z_\odot$ with little, if any, evolution up to $z \simeq 0.3$ (Fukazawa et al. 1998, Renzini 1999). This has been interpreted as evidence supporting the view that the enrichment process in clusters was already completed by that epoch. In general we expect two sources to contribute to the build up of the intracluster medium, infalling IGM and gas stripped from cluster galaxies. In our models these two components have significantly different composition. If the clusters formed at $z \simeq 1$, we expect the IGM to have $\approx 0.1 Z_\odot$ (roughly constant from $z \simeq 1$ to the present), while the galaxies’ ISM has approximately solar composition. The simplest estimate of the resulting metallicity is the geometric mean of these two values (as appropriate for hydrodynamical mixing problems, see Begelman & Fabian 1990), that is $\langle Z \rangle_{icm} = (0.1 \times 1)^{1/2} Z_\odot = 0.32 Z_\odot$, as observed. While this may well be a fortunate coincidence, it is also true that this conclusion lends qualitative support to the

model and the assumptions made.

We make a final point concerning the role of intergalactic dust. The gas phase abundances we have derived do not take into account the possibility that some fraction of heavy elements may be locked up into dust grains. If this were the case, clearly the distributions of metallicities in Figure 6 and 7 would shift towards lower values of Z . In addition, at redshifts where the enrichment is still inhomogeneous, dust associated with regions of high metal concentration may reprocess UV/optical photons into IR radiation and give rise to small scale anisotropies in the Cosmic Microwave Background which may be detectable (Ferrara et al. 1999). Having said this, however, we consider it highly speculative whether dust can survive at all in the hostile environments associated with outflowing superbubbles, where the temperatures are high and the gas has been shocked by SN explosions.

5. Summary

In this paper we have investigated the evolution of the metallicity of the intergalactic medium with particular emphasis on its spatial distribution. We have derived the conditions under which supernova-driven ejection of metals from galaxies can occur. A strong conclusion of our calculations is that if SNe were the only source of kinetic energy for the metals, a highly inhomogeneous distribution would result at any redshift. Under these conditions we would expect most of the volume of the universe to remain at near-primordial composition, with a metallicity $Z \approx 10^{-4}Z_{\odot}$, in contrast with the observational results discussed in the Introduction. Thus, an additional (but yet unknown) physical mechanism must be invoked to mix the metals on scales comparable to the mean distance between the galaxies which are the most efficient pollutants. From this simple hypothesis we have derived a number of testable predictions for the evolution of the IGM metallicity.

Quantitatively, we find that:

1. Metal ejection, or blowout, is inhibited in galaxies with total mass above $M_h \approx 10^{12}(1+z)^{-3/2}M_{\odot}$ due to the combined effects of their larger gravitational field *and* less coherent SN energy deposition.
2. The fraction of metals ejected over the star formation history of the universe is about 50% at $z = 0$. We expect that at the present epoch approximately half of the metals are to be found in the IGM and the average metallicity of luminous matter to be approximately solar.
3. If the ejected metals were homogeneously mixed with the baryons in the universe, the average IGM metallicity would be $\langle Z \rangle = \Omega_Z^{ej}/\Omega_b \simeq 1/25Z_{\odot}$ at $z = 3$. However, due to the spatial inhomogeneity, $\langle Z \rangle$ is actually lower than the mean of the distribution in the diffusive metal-enriched spheres.
4. Metals become homogeneously distributed in the IGM at $z \lesssim 1$, when the metal-enriched

zones overlap, and the spread of the distribution is reduced. We calculate that at $z = 0$ the IGM metallicity is in the range $Z \approx 0.1 \pm 0.03Z_{\odot}$.

5. The uniform metal abundance of intracluster gas from $z \simeq 0.3$ to the present is naturally explained by a mixture of IGM infalling into the cluster and gas stripped from cluster members, with element abundances for both components as predicted by our models.

We should like to thank E. Corbelli, A. Meiksin and B. Nath for useful discussions. YS acknowledges support from the OAArcetri.

REFERENCES

- Babul, A. & Rees, M. J. 1992, MNRAS, 255, 346
- Barlow, T.A., & Tytler, D. 1998, AJ, 115, 1725
- Barnes, J. & Efstathiou, G. 1987, ApJ, 319, 575
- Baugh, C. M., Cole, S., Frenk, C. S., Lacey, C. G., 1998a, ApJ, 498, 504
- Begelman, M. C. & Fabian, A. C. 1990, MNRAS, 244, 26P
- Ciardi, B. & Ferrara, A. 1997, ApJ, 483, L5
- Ciardi, B., Ferrara, A. & Abel, T. 2000a, ApJ, in press (astro-ph/9811137)
- Ciardi, B., Ferrara, A., Governato, F. & Jenkins, A. 2000b, MNRAS, in press (astro-ph/9907189)
- Cowie, L.L., Songaila, A., Kim., T. & Hu, E.M. 1995, AJ, 109, 1522
- Cowie, L.L., Songaila, A., 1998, Nature, 394, 44
- D’Ercole, A. & Brighenti, F. 1999, MNRAS, in press (astro-ph/9907005)
- Dekel, A. 1994, ARA&A, 32, 371
- Edmunds, M. G., & Phillips, S. 1997, MNRAS, 292, 733
- Efstathiou, G., Bond, J.R. & White, S.D.M. 1992, MNRAS, 258, 1P
- Eke, V.R., Cole, S., & Frenk, C.S. 1996, MNRAS, 282, 263
- Ellison, S. L., Lewis, G. F., Pettini, M., Chaffee, F. H. & Irwin, M. J., 1999, ApJ, 520, 456
- Ellison, S.L., Songaila, A., Schaye, J., & Pettini, M. 2000, AJ, submitted
- Ferrara, A. 1998, ApJ, 499, L17
- Ferrara, A., Nath, B. Sethi, S. & Shchekinov, Y. 1999, MNRAS, 303, 301
- Ferrara, A. & Tolstoy, E. 2000, MNRAS, 313, 291

- Franx, M., Illingworth, G., Kelson, D., van Dokkum, P., & Tran, K.-V. 1997, *ApJ*, 486, L75
- Fukawaza, Y., Makishima, K., Tamura, T., Ezawa, H., Xu, H. Ikebe, Y., Kikuchi, K., & Ohashi, T., 1998, *PASJ*, 50, 187
- Fukugita, M., Hogan, C. J. & Peebles, P. J. E. 1998, *ApJ*, 503, 518
- Gnedin, N. Y. & Ostriker, J. P. 1997, *ApJ*, 486, 581
- Gnedin, N. Y. 1998, *MNRAS*, 294, 407
- González Delgado, R.M., Leitherer, C., Heckman, T., Lowenthal, J.D., Ferguson, H.C., & Robert, C. 1998, *ApJ*, 495, 698
- Guiderdoni, G., Hivon, E., Bouchet, F. R., & Maffei, B. 1998, *MNRAS*, 295, 877
- Heckman, T. M., Robert, C., Leitherer, C., Garnett, D. R., & van der Rydt, F. 1998, *ApJ*, 503, 646
- Hellsten, U., Dave, R., Hernquist, L., Weinberg, D. & Katz, N. 1997, *ApJ*, 487, 482
- Kauffmann, G. A. M., 1995, *MNRAS*, 274, 161
- Kovalenko, I. G. & Shchekinov, Yu. 1985, *SovA, Astrophysics*, 23, 578
- Lax, M. 1960, *Rev. Mod. Phys.*, 32, 25
- Lowenthal, J., et al. 1997, *ApJ*, 481, 673
- Lu, L., Sargent, W. L. W., Barlow, T.A., & Rauch, M. 1998, *ApJ*, submitted (astro-ph/9802189)
- MacLow, M.-M. & McCray, R. 1988, *ApJ*, 324, 776
- MacLow, M.-M. & Ferrara, A. 1999, *ApJ*, 513, 142
- Marri, S. & Ferrara, A. 1998, *ApJ*, 509, 43
- McKee, C. F., & Williams, J.P. 1997, *ApJ*, 476, 144
- Miralda-Escudé, J. & Rees, M.J., 1997, *ApJ*, 478, 57L
- Mo, H. J., Mao, S. & White, S. D. M. 1998, *MNRAS*, 295, 319
- Murakami, I. & Babul, A. 1999, *MNRAS*, 309, 161
- Nath, B. & Trentham, N. 1997, *MNRAS*, 291, 505
- Oey, Y. M. S. & Clarke, C. J. 1997, *MNRAS*, 289, 570
- Pettini, M. 1999, in *Chemical Evolution from Zero to High Redshift*, ed. J. Walsh, & M. Rosa (Berlin: Springer), 233
- Pettini, M., Kellogg, M., Steidel, C. C., Dickinson, M., Adelberger, K. L., & Giavalisco, M. 1998, *ApJ*, 508, 539
- Pettini, M., Steidel, C. C., Adelberger, K. L., Dickinson, M., & Giavalisco, M. 2000, *ApJ*, 528, 96
- Press, W. H. & Schechter, P. 1974, *ApJ*, 187, 425
- Rauch, M. et al. , 1997, *ApJ*, 489, 7

- Rauch, M., Haehnelt, M.G., & Steinmetz, M. 1997, *ApJ*, 481, 601
- Renzini, A. 1999, in *Chemical Evolution from Zero to High Redshift*, ed. J. Walsh, & M. Rosa (Berlin: Springer), 185
- Ryan, S. G., Norris, J. E., & Beers, T. C. 1996, *ApJ*, 471, 254
- Salpeter, E. E. & Hoffman, G. L. 1996, *ApJ*, 465, 595
- Sargent, W.L.W., Young, P.J., Boksenberg, A., & Tytler, D. 1980, *ApJS*, 42, 41
- Smith, B.W. 1976, *ApJ*, 211, 404
- Steinmetz, M. & Bartelmann, M. 1995, *MNRAS*, 272, 570
- Tsujimoto, T., Nomoto, K., Yoshii, Y, Hashimoto, M., Yanagida, S. & Thielemann, F.-K. 1995, *MNRAS*, 277, 945
- Tytler, D., Fan, X.M., Burles, S., Cottrell, L., Davis, C., Kirkman, D. & Zuo, L. 1995, in *QSOs Absorption Lines*, ed. G. Meylan (Berlin: Springer), 289
- Barlow, T. A. & Tytler, D. 1998, *AJ*, 115, 1725
- Weil, M. L., Eke, V. R. & Efsthathiou, G. 1998, *MNRAS*, 300, 773
- White, S. D. M. & Frenk, C. S. 1991, *ApJ*, 379, 52
- Zhang, Y., Meiksin, A., Anninos, P., Norman, M. L. 1998, *ApJ*, 495, 63

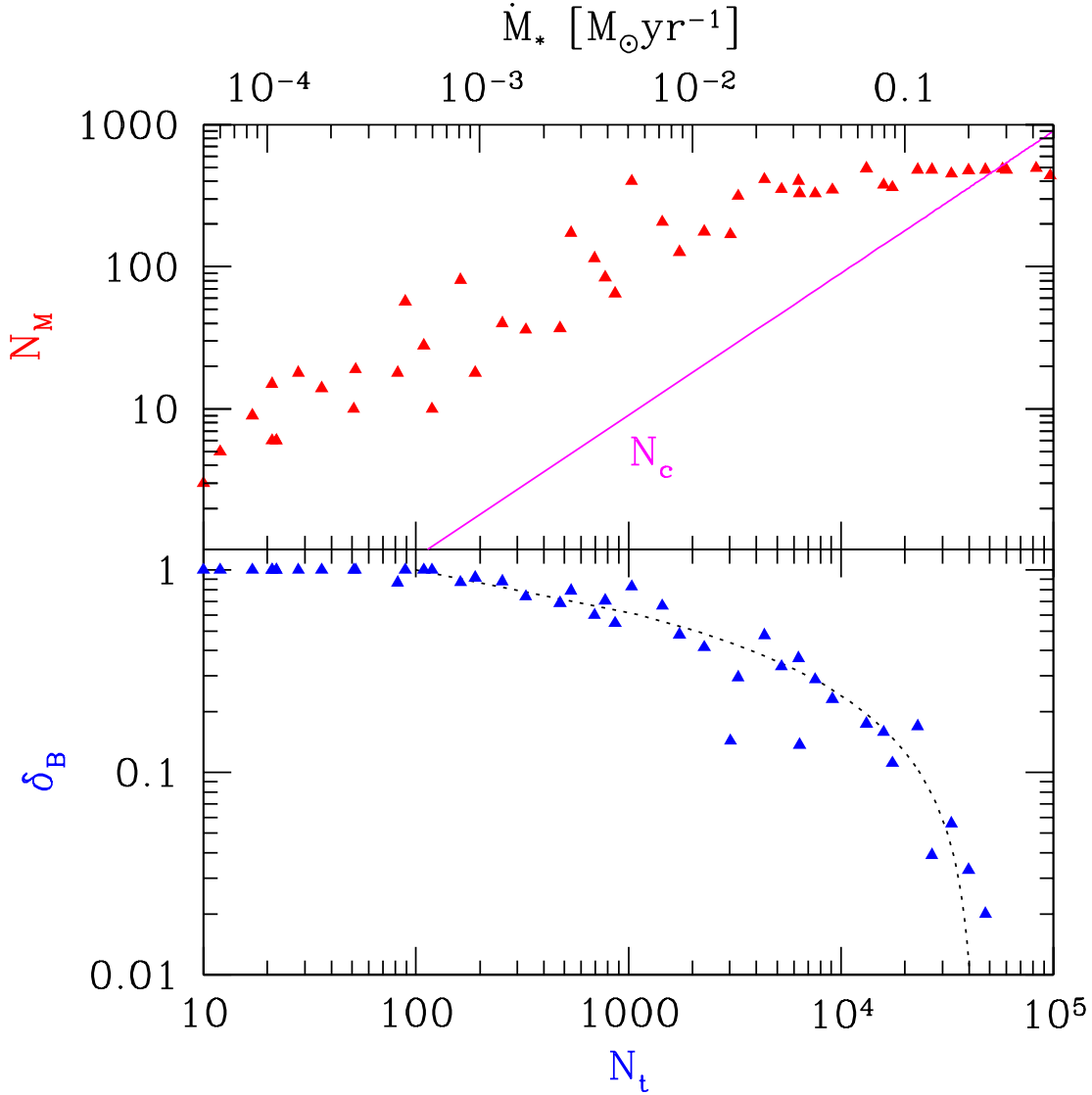


Fig. 1.— *Upper panel:* dependence of the maximum number of SNae in a cluster as a function of the total number of SNae, N_t , produced by a given galaxy in an OB association lifetime as obtained from Monte Carlo simulations; also shown is the critical number of SNae, N_c , for blowout. *Lower panel:* Energy fraction available for blowout, δ_B as a function of the total number of SNae produced by a given galaxy in an OB association lifetime as obtained from Monte Carlo simulations; also shown is an analytical fit to the numerical data.

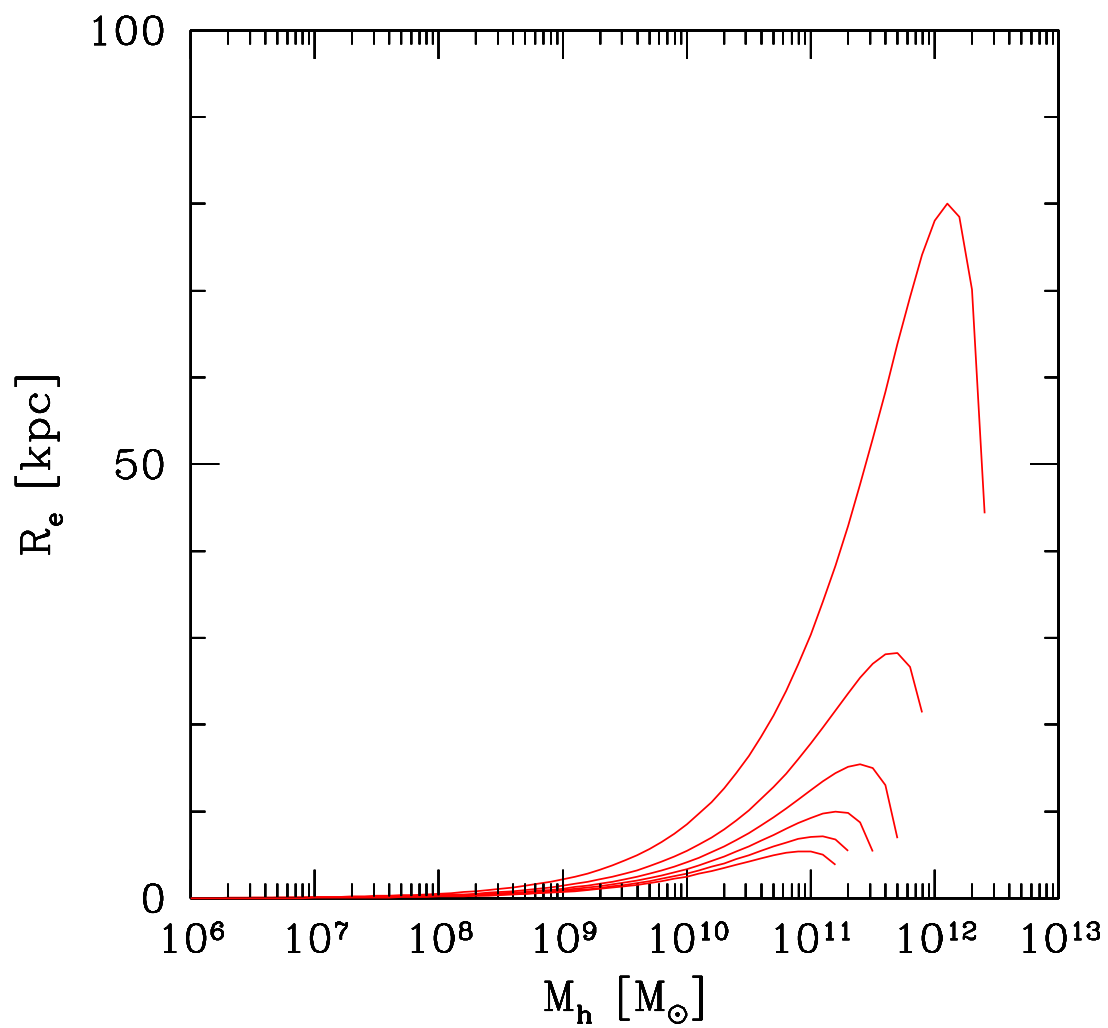


Fig. 2.— Radius of the metal bubble (in physical units) as a function of the halo mass for different virialization redshifts $z = 0, 1, 2, 3, 4, 5$ from the uppermost to the lowermost curve, respectively. The endpoint of each curve denotes the critical mass for blowout.

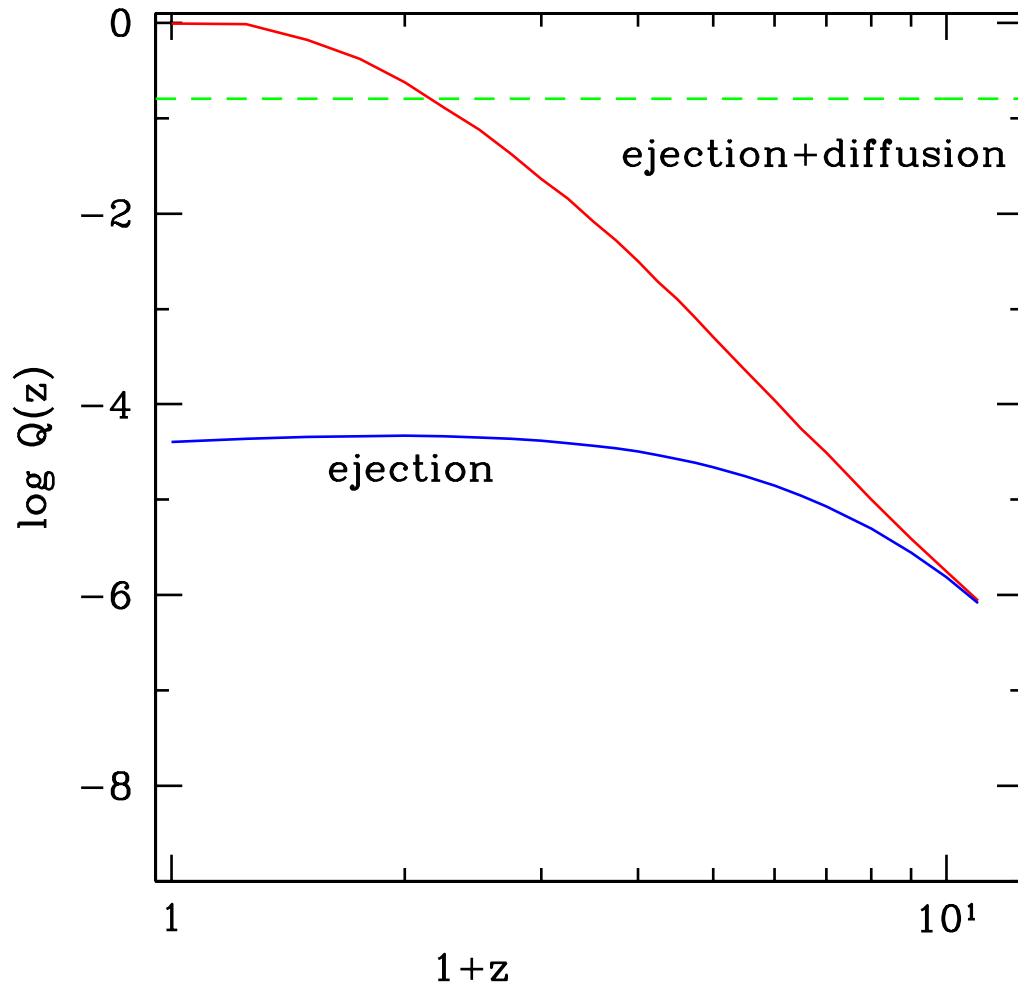


Fig. 3.— Porosity factor of the metal bubbles considering transport by ejection driven by superbubbles (lower curve) and transport due ejection and diffusion processes acting in combination (upper curve). Overlapping of the various bubbles is seen to occur at $z \approx 1$, where $Q(z)$ is equal to the critical value 0.16.

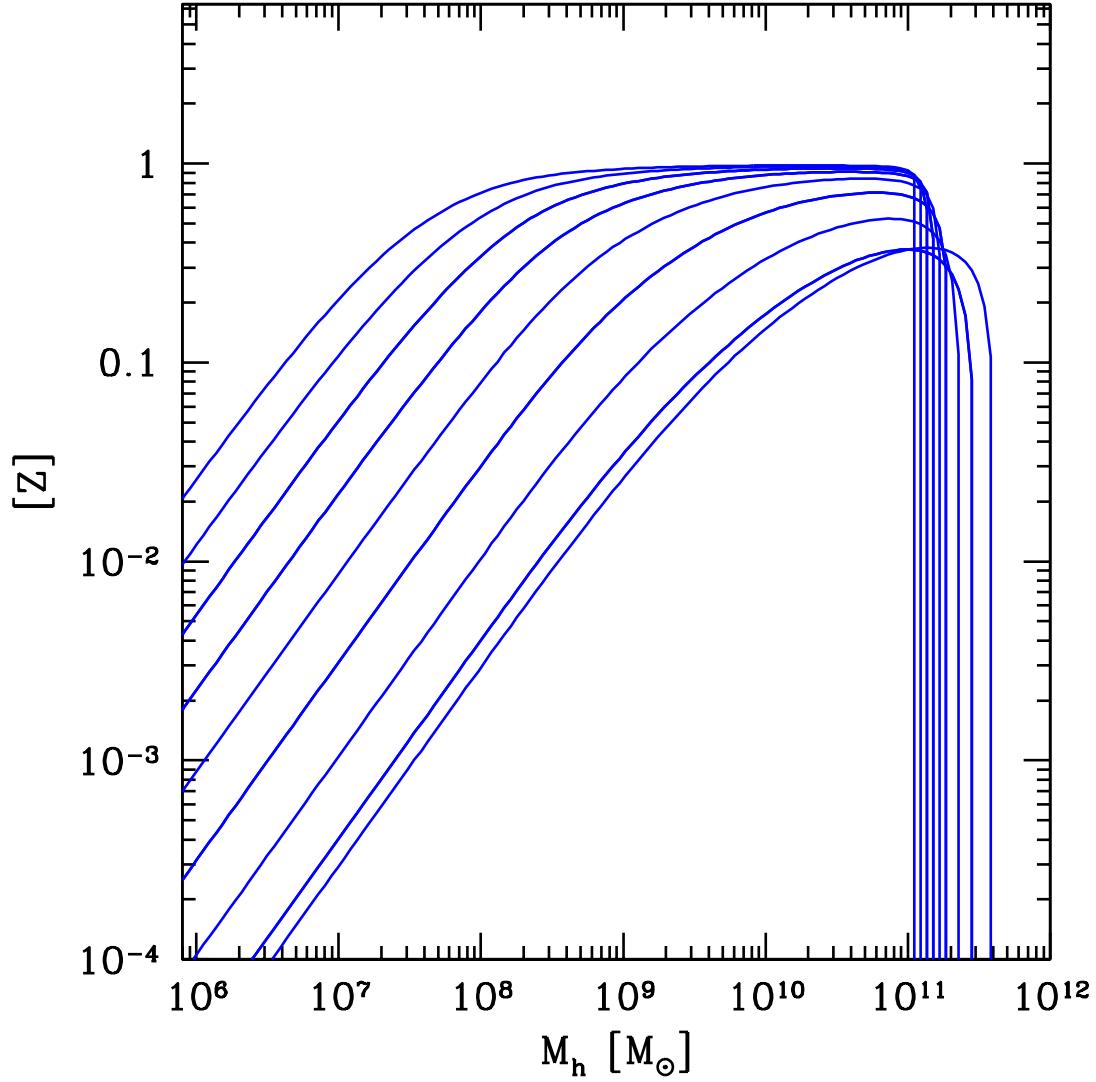


Fig. 4.— Metallicity of diffusive spheres as a function of parent halo mass for redshifts $z = 0, 0.5, 1, 1.5, 2, 2.5, 3, 3.5, 4$ from the bottom to the top curves, respectively. The curves shown are for the case where the initial metallicity of the hot gas in the superbubbles is solar.

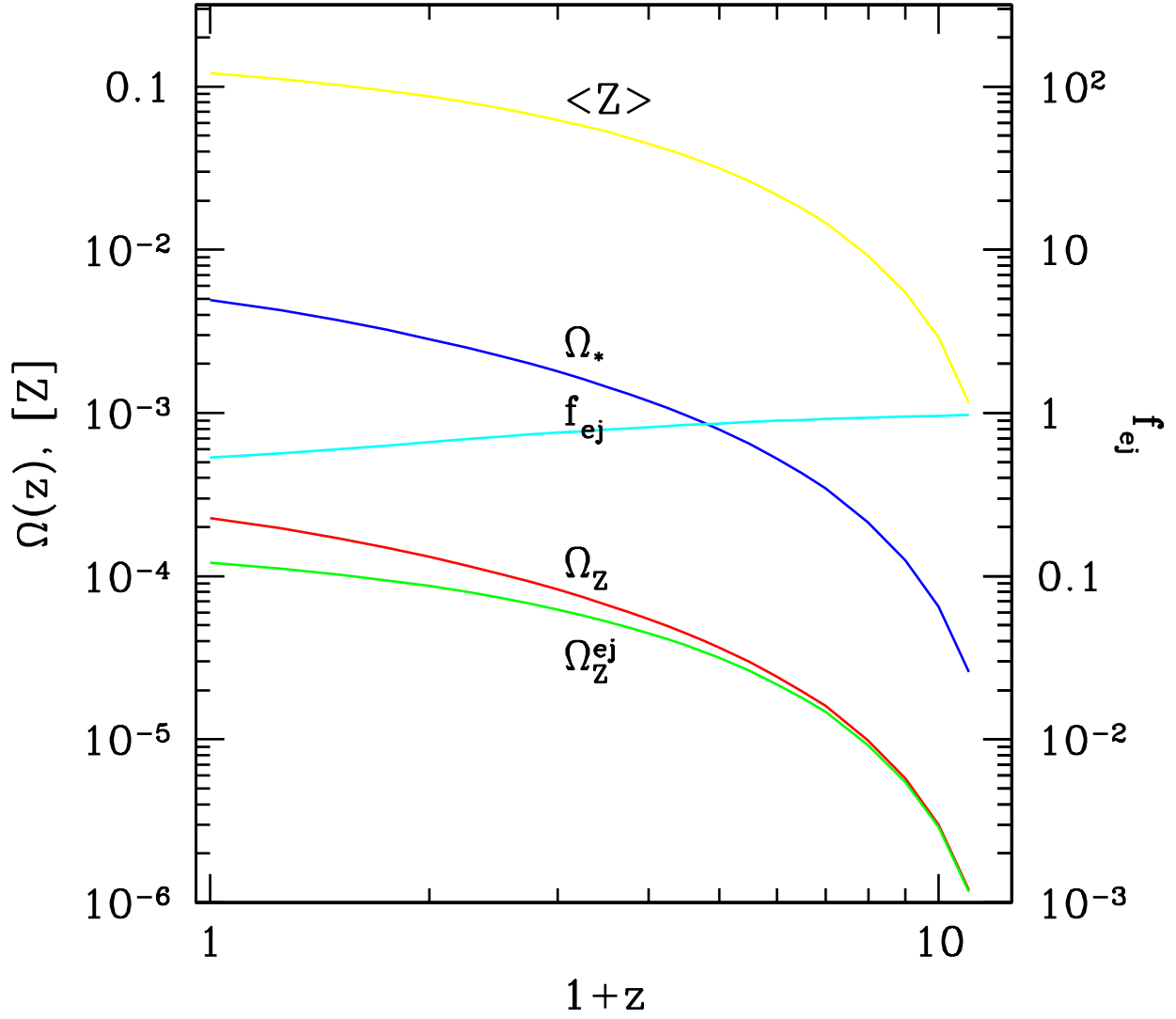


Fig. 5.— Redshift evolution of density parameter for produced (Ω_Z) and ejected (Ω_Z^{ej}) metals, stars (Ω_*), cosmic metal escape fraction (f_{ej}), and average IGM metallicity ($\langle Z \rangle$) for the SCDM model.

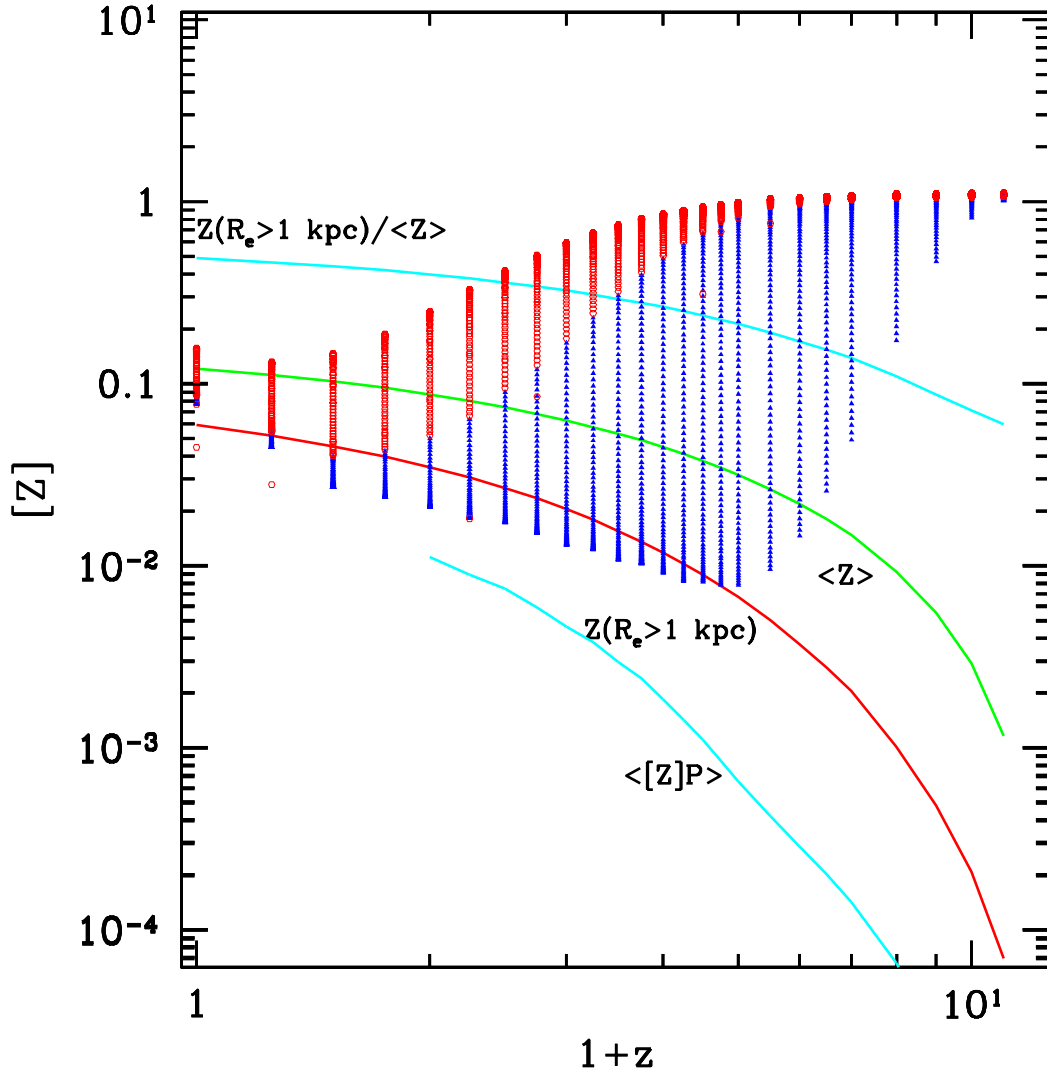


Fig. 6.— Redshift evolution of the IGM metallicity distribution in the SCDM model. Also shown are the average IGM metallicity, $\langle Z \rangle$, the contribution from objects with large metal-enriched spheres, $Z(R_e > 1 \text{ kpc})$, the ratio of the two, and the covering factor-weighted metallicity, $\langle [Z]P(z) \rangle$. The initial value of the hot gas metallicity is Z_{\odot} (standard case).

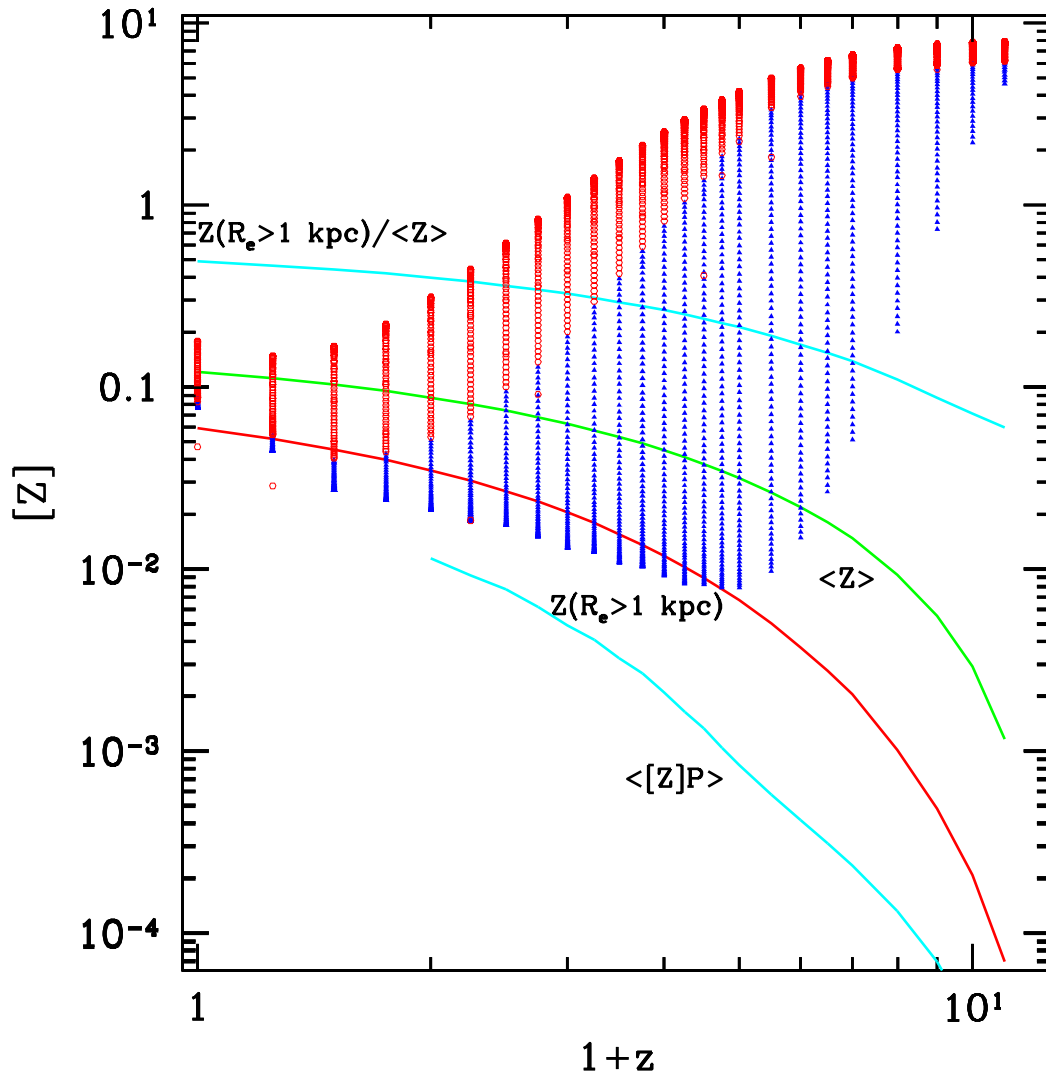


Fig. 7.— Same as Fig. 6, but for initial value of the hot gas metallicity $8 Z_{\odot}$.

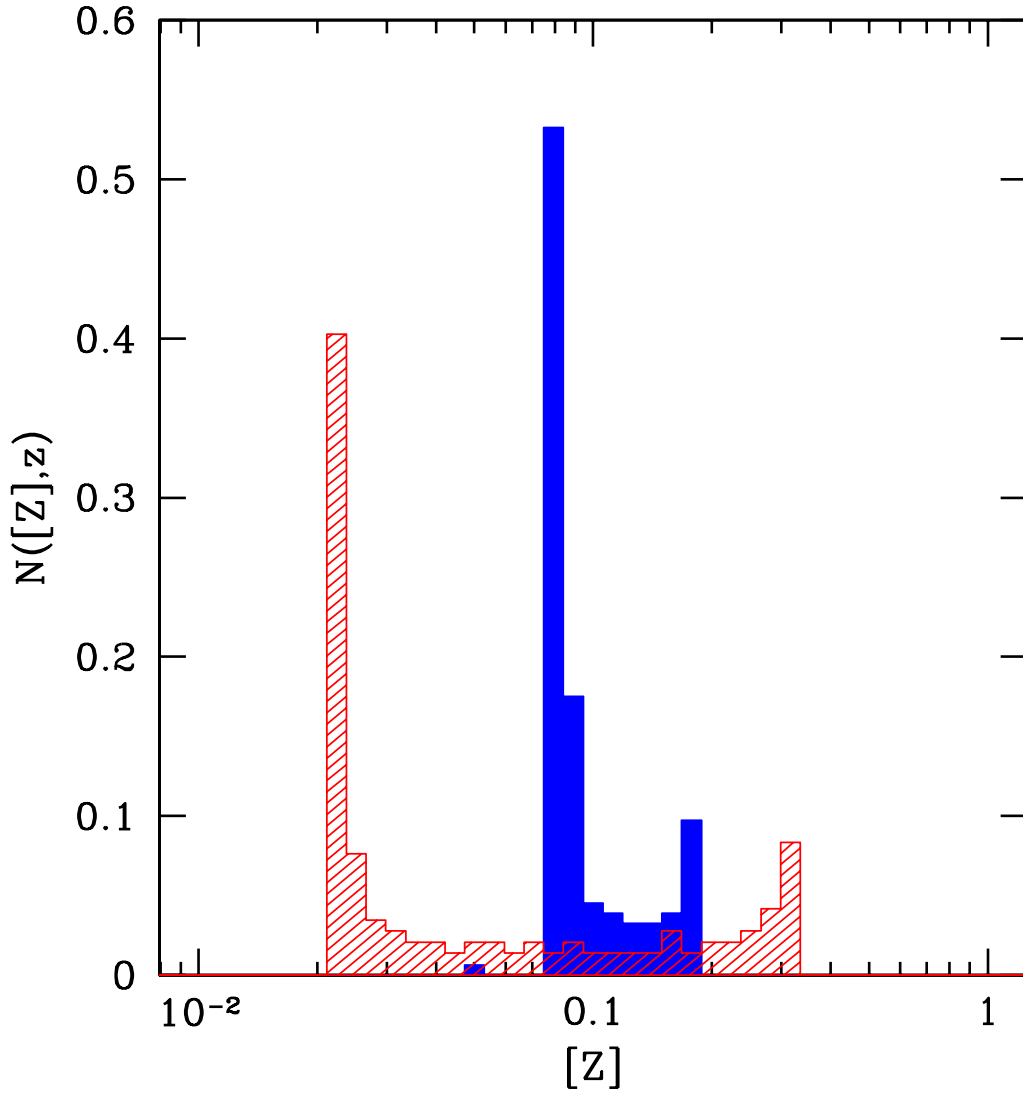


Fig. 8.— IGM metallicity distribution function for the SCDM model at redshift $z = 1$ (obliquely dashed) and $z = 0$ (solid). Both histograms are normalized to unity; the initial value of the hot gas metallicity is Z_{\odot} .